Stem Cell Research & Therapy

RESEARCH Open Access

Hypoxia-preconditioned WJ-MSC spheroid-derived exosomes delivering miR-210 for renal cell restoration in hypoxia-reoxygenation injury

Reyhaneh Toghiani[1], Vajihe Azimian Zavareh[2], Hanyieh Najafi[1], Mina Mirian[3], Negar Azarpira[4], Samira Sadat Abolmaali[1], Jaleh Varshosaz[5] and Ali Mohammad Tamaddon[1,6*]

Abstract

Background Recent advancements in mesenchymal stem cell (MSC) technology have paved the way for innovative treatment options for various diseases. These stem cells play a crucial role in tissue regeneration and repair, releasing local anti-inflammatory and healing signals. However, challenges such as homing issues and tumorigenicity have led to exploring MSC-exosomes as a promising alternative. MSC-exosomes have shown therapeutic potential in conditions like renal ischemia-reperfusion injury, but low production yields hinder their clinical use.

Methods To address this limitation, we examined hypoxic preconditioning of Wharton jelly-derived MSCs (WJ-MSCs) 3D-cultured in spheroids on isolated exosome yields and miR-21 expression. We then evaluated their capacity to load miR-210 into HEK-293 cells and mitigate ROS production, consequently enhancing their survival and migration under hypoxia-reoxygenation conditions.

Results MiR-210 overexpression was significantly induced by optimized culture and preconditioning conditions, which also improved the production yield of exosomes from grown MSCs. The exosomes enriched with miR-210 demonstrated a protective effect by improving survival, reducing apoptosis and ROS accumulation in damaged renal cells, and ultimately promoting cell migration.

Conclusion The present study underscores the possibility of employing advanced techniques to maximize the therapeutic attributes of exosomes produced from WJ-MSC spheroid for improved recovery outcomes in ischemia-reperfusion injuries.

Keywords Wharton jelly-derived mesenchymal stem cells, Hypoxia preconditioning, Exosome, 3D culture, Renal ischemia-reperfusion injury

*Correspondence:
Ali Mohammad Tamaddon
amtamadon@sums.ac.ir; amtamadon@gmail.com
[1]Department of Pharmaceutical Nanotechnology, Center for Nanotechnology in Drug Delivery, Shiraz University of Medical Sciences, Shiraz, Iran
[2]Department of Plant and Animal Biology, Faculty of Biological Sciences and Technology, University of Isfahan, Isfahan, Iran
[3]Department of Pharmaceutical Biotechnology, School of Pharmacy and Pharmaceutical Sciences, Isfahan University of Medical Sciences, Isfahan, Iran
[4]Transplant Research Center, Shiraz University of Medical Sciences, Shiraz, Iran
[5]Department of Pharmaceutics, School of Pharmacy and Pharmaceutical Sciences, Isfahan University of Medical Sciences, Isfahan, Iran
[6]Department of Pharmaceutics, School of Pharmacy, Shiraz University of Medical Sciences, Shiraz, Iran

Introduction

Acute kidney injury (AKI) is a significant clinical problem mainly caused by renal ischemia resulting in impaired oxygen supply to the kidneys [1]. Ischemia followed by reperfusion causes further renal damage due to cytokine release and generation of free radicals and reactive oxygen species (ROS) [2]. Even though reperfusion is needed to restitute oxygen and nutrient requirements of kidney cells, it can lead to systematic inflammatory responses and tissue damage known as ischemia-reperfusion injury (IRI) [3, 4].

Recently, much research has been done on the therapeutic effect of mesenchymal stem cells (MSCs) and their secretome for IRI treatment. MSCs can reduce or restrict ischemic tissue injury via directly homing to injured tissue and regeneration of damaged cells or indirectly by paracrine/endocrine factors secretion [5]. However, systematic administration of MSCs causes localization mainly in other tissues such as the lungs [6, 7]. Also, local injection of MSCs exhibits poor delivery to ischemic tissues, attenuating their therapeutic effects [8]. On the other hand, MSC secretome or extracellular vehicles (EVs) such as exosomes are increasingly being explored in various experimental conditions, such as neurodegenerative disorders [9], bone and cartilage injuries [10], cardiovascular [11], and kidney diseases [12], wound healing [13], and tissue or organ fibrosis [14]. The sorting and packaging of cargo into exosomes are tightly regulated processes that involve various cellular pathways, including the endosomal sorting complex required for transport (ESCRT) machinery and other ESCRT-independent mechanisms [15]. Exosomes play a crucial role as mediators of cell-to-cell communication [16], due to specific membrane molecules that facilitate their interaction with cells, leading to cargo delivery through endocytosis or direct fusion with the cell membrane [17]. MSC-derived exosomes have gained significant attention for tissue repair and regenerative medicine. They are less likely to trigger an immune response compared to whole MSCs. This reduces the risk of rejection or adverse immune reaction when used for therapy [18, 19]. So, MSC-derived exosomes can home in on the injured tissue due to their small size and molecular cargo. This enables targeted delivery of therapeutic molecules to the site of IRI, potentially improving the therapeutic effect [20, 21]. Additionally, MSC-derived exosomes have anti-inflammatory and immunomodulatory properties, which can help suppress excessive inflammation associated with IRI and promote tissue healing [22]. They contain a diverse range of bioactive molecules, including growth factors, cytokines, regulatory molecules, and microRNAs [23]. These molecules can modulate various cellular processes, such as inflammation, apoptosis, and tissue repair, contributing to the mitigation of IRI. Ultimately, unlike whole MSCs, exosomes have a lower potential for tumorigenicity which is an important consideration in cell-based therapies [24].

While MSC-derived exosome exhibits therapeutic potential for various diseases, their low yield hinders their practical therapeutic use. The exosome yield is influenced by the culture condition and purification process [25]. Several reports have demonstrated that a three-dimensional (3D) culture yields a higher quantity of exosomes than the conventional two-dimensional (2D) system [26]. Additionally, when compared to exosomes generated through 2D culture, those originating from 3D culture exhibit enhanced therapeutic effects through the transfer of specific cargoes [27]. In addition, much research has shown that exosomes obtained from the culture media in which MSCs have been grown under hypoxic conditions carry molecular cargos released by the MSC in response to the environment with potential therapeutic effects in IRI [28]. Among cargos, microRNAs (miRNAs or miRs) are a member of noncoding RNA [29, 30]. These molecules are known as the transcriptional regulators of many biological processes in cell fate, such as stress response, proliferation, and death [31]. miR-210 is a major hypoxemia induced through hypoxia conditions in different cells and is illustrated as a hypoxia genetic signature [32]. Several research has shown that miR-210 has angiogenic [33–35] and anti-apoptotic [36, 37] effects in ischemia conditions. Therefore, by combining hypoxic preconditioning of MSC to enhance miR-210 expression and 3D culture to boost the yield of exosome secretion, we hypothesized the exosome derived from a hypoxic condition in the 3D culture of Wharton's jelly MSCs (WJ-MSCs) would mitigate ischemic injury. To this aim, we isolated exosomes from WJ- MSCs subjected to hypoxic preconditioning and spheroid 3D system. We then assessed their capacity to load up miR-210 within HEK-293 cells and to mitigate ROS production, enhancing their survival under hypoxia-reoxygenation conditions.

Materials and methods

WJ-MSCs isolation and culture

WJ-MSCs were isolated and expanded according to the previously reported methods [38, 39]. Human umbilical cord samples ($n=3$) were aseptically collected from the Obstetric Department affiliated with Shiraz University of Medical Sciences (SUMs), Shiraz, Iran. Infectious samples were excluded by performing hepatitis C and B virus (HCV, HBV) and human immunodeficiency virus tests. The tissues were stored in PBS solution supplemented with 1% antibiotic–antimycotic solution on ice. After removing blood vessels, the Wharton's jelly was scraped from the amnion and dispensed into 2 to 3-mm pieces. These tissue pieces were explanted and cultured

in DMEM-F12 supplemented with 10% FBS and 1% antibiotic-antimycotic solution at 37 °C with 5% CO2.

Commercial osteocyte and adipocyte differentiation media (Bonyakhteh, Iran) were used for evaluating the cell differentiation potential. After 14 and 21 days, the samples were fixed and stained with Alizarin Red and Oil Red O staining to confirm the cell differentiation potential.

To determine the phenotype of cell-surface antigens, cells from the third passage were stained with FITC-conjugated antibodies (BioLegend, San Diego, CA, USA) specific for hematopoietic lineage markers CD34 and CD45, and stromal surface markers CD90 and CD44. The stained cells were resuspended in PBS before being analyzed with a FACSCalibur flow cytometer (Becton Dickinson, USA). At least 10,000 events were recorded for each sample as similarly reported elsewhere [40].

WJ-MSC spheroid formation and hypoxia conditioning

We used a straightforward method for hypoxic preconditioning of WJ-MSCs by standard incubators (37 °C with 5% CO_2) [41]. Accordingly, WJ-MSCs (passage number 2–5) were isolated from Wharton jelly and seeded in 4 wells of a 6-well plate at the density of 2×10^5 cells/well. When cells were grown to 70–80% confluence, we put an oxygen absorber pack (Bihava, Iran, Tehran) in one of the empty wells and in the other empty well, an oxygen indicator (Anaerotest Strips, Merck, Germany) was located. The color change on the reaction zone of the indicator test strip provides a clear visual indication of the oxygen levels (<1%) in the environment, making it easy to justify hypoxia conditioning. For exchanging gas inside the 6-well plate, two plastic spacers were placed in parallel crossing the top of any three wells. Then, the assembled cell culture plate was put into a vacuum bag. Finally, the bag containing the cell culture plate was evacuated and sealed by a plastic sealing machine. This package was inserted in a standard incubator for different times (3, 6, 12, and 24 h). After hypoxic preconditioning, WJ-MSCs were trypsinized and immediately used to form spheroids at a density of 1×10^6 cells per 25 cm^2 flask coated by 1% low melt agarose for 24 h [42]. For determining cell viability under hypoxia conditioning, the spheroids were subjected to the acridine orange (AO) / propidium iodide (PI) double staining assay [43]. Briefly, the cell spheroids, formed by the hanging drop method (7500 cells/drop) under normoxia and hypoxia conditions for 24 h, were washed with PBS, and then 10 µl fresh AO/PI stain solution (10 µg/ml AO, 50 µg/ml PI) were added. After 15 min, the spheroid was washed with PBS and examined under fluorescence microscopy (FV1000 viewer Olympus, Japan).

Exosome isolation and characterization

After 24 h following spheroid formation, the medium was replaced by a serum-free culture medium to exclude FBS supplementation. After incubation of spheroids in serum-free medium for 48 h, the supernatant was collected by centrifuging at 3,000 rpm for 10 min by Hettich Centrifuge (Model Rotofix 32, Germany), and exosomes were separated using Exocib exosome isolation kit (Cibbiotech, Tehran, Iran) according to the manufacturer instruction. Briefly, the cell culture supernatant was centrifuged at 300 g for 10 min to remove residual debris. Subsequently, it was filtered via a 0.22 µm sterile syringe filter (CA syringe filter, single pack, USA) and Exocib reagent A was then added to the supernatant. After 5 min vortex and overnight incubation at 4 °C, the mixture was centrifuged at 3,000 g for 40 min at 4 °C. Finally, the separated exosome pellets were resuspended in Exocib reagent B and stored at −70 °C before use.

The total protein level of lysed exosome (0.5% triton x-100) was analyzed by the BCA assay kit (Kiazist, Iran). The average exosome yield was 1790 µg/ml from 50 ml of culture supernatant. Also, the isolated exosomes were subjected to morphological assessment using field emission scanning electron microscopy (FESEM; QUANTA FEG-450, FEI, USA). To prepare a sample for FESEM imaging, 20 µl of exosome suspension was air-dried at room temperature and subsequently coated with a thin layer of gold. Then, it was examined using an accelerating voltage of 20 keV. Additionally, isolated exosome size distribution was determined by a dynamic light scattering (DLS) nanoparticle analyzer (Horiba, sz-100, Japan). For sample preparation, 50 µl of sample suspension was diluted to 1 ml phosphate buffer (pH 7.4) before analysis. The CD markers of exosomes such as CD9, CD63, and CD81 protein percent were detected by flow cytometry assay with a FACSCalibur flow cytometer (Becton Dickinson, USA).

In-vitro hypoxia-reoxygenation (H/R) treatment

HEK-293 cells were plated in a 6-well plate at a density of 3.5×10^5 cells/well in a high glucose DMEM medium containing 10% fetal bovine serum. After 70% confluence was reached, an oxygen-glucose deprivation (OGD) experiment was conducted to simulate ischemia in vitro. Briefly, the medium was replaced by low glucose DMEM, and the cells were incubated in a hypoxic condition for 12 h. Then, the vacuum bag was opened, and the cells were transferred to normal conditions during reoxygenation for 24 h. During reoxygenation, the cells were treated with different preconditioned WJ-MSC-derived exosomes (WJ-MSC-$EX^{miR-210}$) (50, 100, and 150 µg/ml). Cell viability was determined by trypan blue staining. The cells cultured in various hypoxic times were suspended and stained with 0.4% trypan blue solution.

Then, the number of living and dead cells was counted by hemocytometry.

In vitro cellular uptake of coumarin-6 labeled exosomes (Ex-C6)

To evaluate how well the exosomes were taken up by cells, a process involving fluorescent labeling was conducted using coumarin-6, a lipophilic fluorescent dye [44, 45]. Briefly, equal volumes of exosomes dispersed in phosphate-buffered saline (PBS) and ethanolic coumarin-6 solution at a concentration of 250 µg/ml were mixed and incubated at 37 °C for 30 min. Both the coumarin-6-labeled exosomes (Ex-C6) and a solution of free ethanolic coumarin-6 were then incubated with IRI model HEK-293 cells in a 6-well plate, with a total of 2×10^5 cells per well for 4 h. Following the incubation period, the cells were washed with PBS and then fixed with a 4% paraformaldehyde solution. After another rinse with PBS, the cells were stained with DAPI, a fluorescent nuclear stain. Imaging of the cells was then performed using fluorescence microscope (FV1000 viewer Olympus, Japan). Finally, the images obtained were analyzed using Image J software.

RNA extraction and quantitative real-time polymerase chain reaction (RT-PCR)

Total RNA was extracted from exosomes and cell specimens using TRIzol reagent (Invitrogen, Paisley, UK). Briefly, 3 µg of total RNA was converted to cDNA according to the manufacturer's instructions (Royan stem cell, Tehran, Iran). The Real-time PCR was conducted using 1X SYBR® Green PCR Master Mix (Applied Biosystems, California, USA). Finally, the expression of assessed genes was normalized relative to U6 (Seq (5−3) AAGGATG ACACGCAAAT) as a reference gene for miR-210 (Seq (5−3) CCTGTGCGTGTGACAG), and quantification of gene expression was analyzed via ABI Step One System (Applied Biosciences, Foster City, CA). The superscript method was used to calculate the relative expression.

For assessing miR-210 expression in HEK 293 cells, RNA was extracted from 10^6 cells treated with exosomes isolated from normoxic or hypoxic WJ-MSCs and compared to untreated control cells. Subsequently, cDNA was synthesized, and RT-PCR was conducted as previously explained.

MTT cell viability assay

Cell viability was measured using the 3-(4,5-dimethyl-2-thiazolyl)-2,5-diphenyl-2-H-tetrazolium bromide (MTT) assay. Briefly, OGD-conditioned HEK cells (10^4 cells/well) were seeded in a 96-well plate and treated with different concentrations of WJ-MSC-$EX^{miR-210}$ for 24, 48, and 72 h. After treatment of hypoxia and subsequent normoxia renal cells by WJ-MSC-$EX^{miR-210}$ for 24 h, the MTT solution (0.5 mg/ml, 20 µl) was added, and cells were incubated for 4 h at 37 °C. Subsequently, 100 µl DMSO was added to each well to solubilize the formazan reaction product with gentle shaking for 5 min. The optical density (OD) was read at 570 nm on a microplate reader (BioTek, USA). Experiments were conducted in triplicate and survival of the untreated control group was defined as 100%, and that of the H/R group was expressed as the percentage of the control group.

Scratch test

The HEK293 cells were seeded at 3.5×10^5 cells/well into 6-well plates, and when they reached a confluence of 80%, a hypoxia condition was applied. Subsequently, a scratch line was made across each well using a sterile plastic of 100 µl micropipette tip. After washing cells twice with PBS, serum-free media containing different concentrations of WJ-MSC-$EX^{miR-210}$ was added to wells. Images for each scratch were taken at 0, 6, 12, 24, 48, and 72 h. Cell migration was measured by calculating the percent change in wound area over time compared to the wound area at zero time by Image J software (open source).

Intracellular ROS assay

Cellular reactive oxygen species (ROS) levels were quantified using 2,7-dichlorodihydrofluorescein diacetate (H2DCFDA; Sigma). This dye, a stable nonpolar compound, easily permeates cells, converting to DCFH. In the presence of peroxidase, intracellular ROS transforms DCFH into the highly fluorescent DCF. The resulting fluorescence intensity is thus indicative of cellular ROS production. For this assay, H/R renal cells were treated with different exosome concentrations. After 24 h, cells were incubated with 10 mM H2DCFDA for 30 min at 37 °C. Then, cells were washed twice with PBS and immediately evaluated using a flow cytometer in the emission wavelength of 538 nm (BD Biosciences, USA).

Apoptosis assay

Cell apoptosis was assessed using the Annexin V-FITC/PI apoptosis detection kit (Thermo Fisher Scientific). Briefly, the hypoxia/reoxygenation-conditioned HEK-293 cells were treated with three concentrations of WJ-MSC-$EX^{miR-210}$ (50,100, and 150 µg/ml) for 24 h. Then, the treated cells, as well as untreated hypoxia/reoxygenation-conditioned and normoxic control cells were trypsinized (Bioidea, Tehran, Iran) and collected. After washing with PBS, each tube of cells was suspended in 200 µl of binding buffer containing 5 µl of Annexin V-FITC, and 5 µl of PI. Subsequently, tubes were incubated in the dark for 20 min. Finally, stained cells were analyzed using Flow Cytometry (BD Biosciences, USA).

Statistical analysis

All data are expressed as mean ± SD from a minimum of three independent experiments. Statistical analyses were conducted using GraphPad Software 7.0. Student's t-test was employed for comparisons between two groups, while one-way or two-way ANOVA with Tukey's test was used for multiple comparisons. A significance level of $P<0.05$ was considered statistically significant.

Results

WJ-MSC isolation and characterization

WJ-MSCs grew like plastic adherent cells under in vitro culture conditions with a fibroblast-like morphology (Fig. 1a). After differentiation toward osteogenic and adipogenic lineages, the presence of calcium deposition was confirmed with Alizarin Red and lipid vacuoles was revealed by Oil Red O, respectively (Fig. 1b). According to the flow cytometry findings, WJ-MSCs expressed stromal markers (CD44 and CD90), but not hematopoietic markers (CD45 and CD34) (Fig. 1c). These findings are consistent with the literature [46]. In reality, the flow cytometry results showed that recovered cells were negative for CD45 (0.5%) and CD34 (0.24%) and positive for CD44 (91%) and CD90 (89.1%).

Three-dimensional (3D) WJ-MSC culture under hypoxia conditioning

Two-dimensional (2D) WJ-MSCs were cultured in a standard condition as monolayers for passaging up to P5 (Fig. 2a). Figure 2b shows WJ-MSC spheroids with approximately 1×10^6 cells formed via forced aggregation in a non-adherent flask coated by low melting agarose 1% in 24 h. To explore the effect of hypoxic preconditioning on cell viability in 3D spheroids, AO and PI double staining were employed for WJ-MSC cultured under normoxic and hypoxic conditions (Fig. 2c). AO permeates live and dead cells, producing green fluorescence upon binding to nucleated cells. Conversely, PI only enters cells with injured membranes, staining dead cells and emitting red fluorescence. When both AO and PI are applied, the fluorescence of AO is quenched by PI through fluorescence resonance energy transfer. Consequently, live nucleated cells exhibit green fluorescence, while dead nucleated cells exhibit red fluorescence. [47] The spheroid images were analyzed using the Image J software. Figure 2d shows the hypoxic condition could increase cell viability in 3D spheroids (88% vs. 62% for hypoxic precondition and normoxic, respectively).

In addition, we compared exosome secretion from 5×10^5 WJ-MSCs cultured in a conventional monolayer (2D) with that from cells cultured in 3D spheroids. After 24 h of cell seeding and spheroid formation, the medium was replaced by a serum-free medium, and the secreted exosomes were harvested after 48 h. As a preliminary test, the BCA assay was performed to determine the total exosome protein. As shown in Fig. 2e, the yield of exosomes isolated from spheroids was significantly higher than 2D culture (665 vs. 230 µg/ml) ($P<0.05$).

Exosome characterization

WJ-MSCs were seeded under normoxia and hypoxia conditions, and exosomes were isolated from serum-free media after 48 h incubation. Exosome markers, including CD9, CD63, and CD81 were verified by flow cytometry, confirming exosome identity. In addition, characteristic analysis illustrated that the average size of WJ-MSC-derived exosomes was 57.6 ± 2.3 nm, which was in line with the reported range of exosome size [48]. Furthermore, we assessed the exosomes with electron microscopy and then confirmed the size range of less than 100 nm with spherical morphology (Fig. 3).

Induction of miR-210 cargo in hypoxia-preconditioned WJ-MSC-derived exosomes

The composition and functionality of exosomes are contingent upon the cell of origin, implying that intercellular communication via exosomes is a dynamic system adaptable to the conditions of the producing cell. Alterations in oxygen concentration impact several unique features of stem cells, enabling the delivery of biological information through internalization by neighboring or distant cells. Given this premise, to determine the optimal duration of hypoxic preconditioning for WJ-MSCs and its effect on cell viability before spheroid formation in a 2D culture setup using a 6-well plate, the preconditioning of WJ-MSCs at a different time (3, 6, 12, 24, 48, and 72 h) of hypoxia exposure was investigated. As shown in Fig. 4a, hypoxia treatment induced decreased viability of WJ-MSC cells in a time-dependent manner. So, 48 and 72 h hypoxia conditions were ignored because of a significantly reduced (more than 50%) cell viability ($P<0.0001$). Subsequently, after spheroid formation, the miR-210 expression, as a biomarker of hypoxic condition, in exosome-derived WJ-MSCs was analyzed by RT-PCR at other times (3, 6, 12 and 24 h). As shown in Fig. 4b, the miR-210 expression significantly increased at 24 h with a 145.5 ± 14.0-fold change compared to the normoxia condition ($P<0.0001$).

Therefore, 24 h hypoxia was selected for WJ-MSC preconditioning.

In vitro cellular uptake of hypoxia preconditioned WJ-MSC-derived exosomes and overexpression of miR-210 in them

The capacity for uptake and efficient internalization of exosomes by HEK-293 cells was analyzed via exosome labeling with coumarin6 (EX-C6). In accordance Fig. 5a, the green fluorescent panel illustrated that EX-C6 exhibited increased cellular uptake in HEK-293 cell

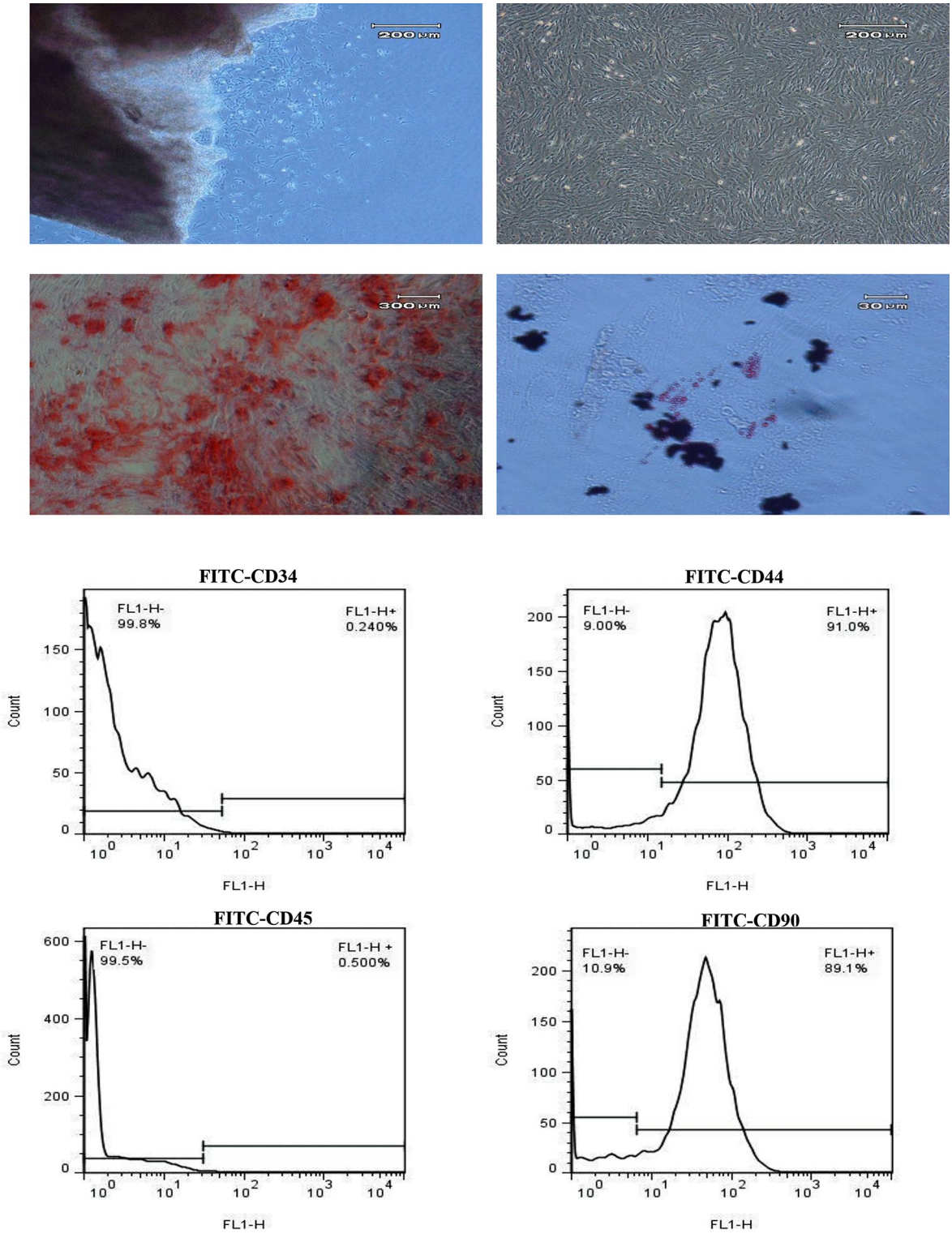

Fig. 1 Characterization of Wharton's jelly-derived mesenchymal stem cells (WJ-MSCs). (**a**) The morphology of WJ-MSCs, (**b**) differentiation of WJ-MSCs to osteocytes and adipocytes, as confirmed by Alizarin Red and Oil Red O, respectively, and (**c**) the flow cytometry results for CD45, CD34, CD44, and CD90

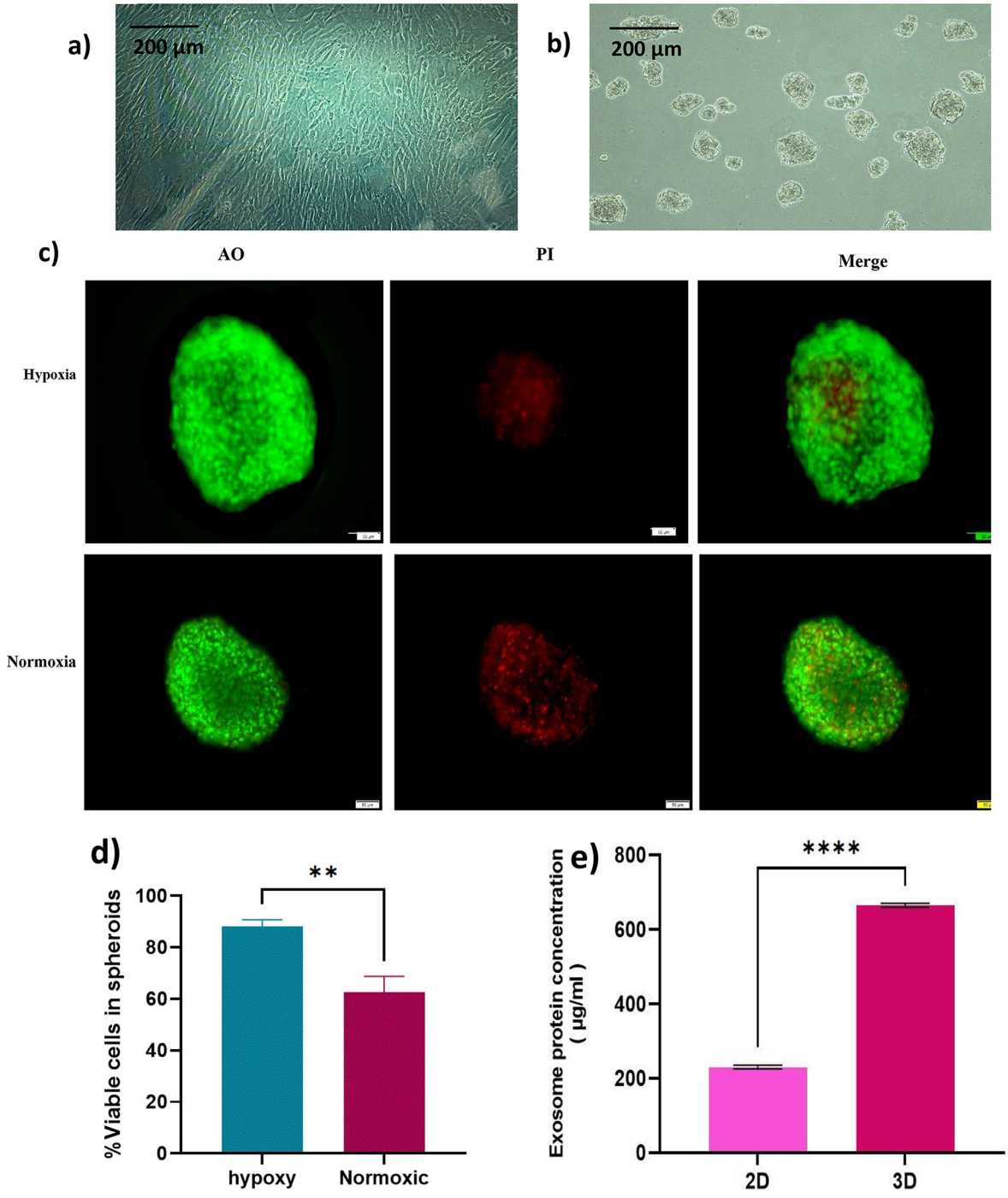

Fig. 2 3D culture increases cell viability and exosome secretion (**a**) conventional 2D WJ-MSC. (**b**) WJ-MSC 3D culture and spheroid formation (**c**) AO and PI staining of cell spheroids (7500 cells per spheroid) (**d**) viability of spheroids according to double staining of spheroids by AO and PI and using image J software. (**e**) BCA assay of exosome proteins isolated from 5×10^5 WJ-MSCs seeded as 2D and 3D culture. (**$P<0.01$, ****$P<0.0001$)

lines, indicating enhanced internalization of exosomes compared to free C-6. The increased cellular uptake of exosomes may be primarily attributed to their effective cellular internalization mechanisms, involving both clathrin-mediated endocytosis and micropinocytosis [49].

H/R kidney cell viability and migration enhanced by hypoxia preconditioned WJ-MSC- derived exosomes (WJ-MSC-EX$^{miR\text{-}210}$)

The effect of WJ-MSC-EX$^{miR-210}$ on the viability of hypoxia-reoxygenation conditioned kidney cells was analyzed by MTT assay. The result showed that the

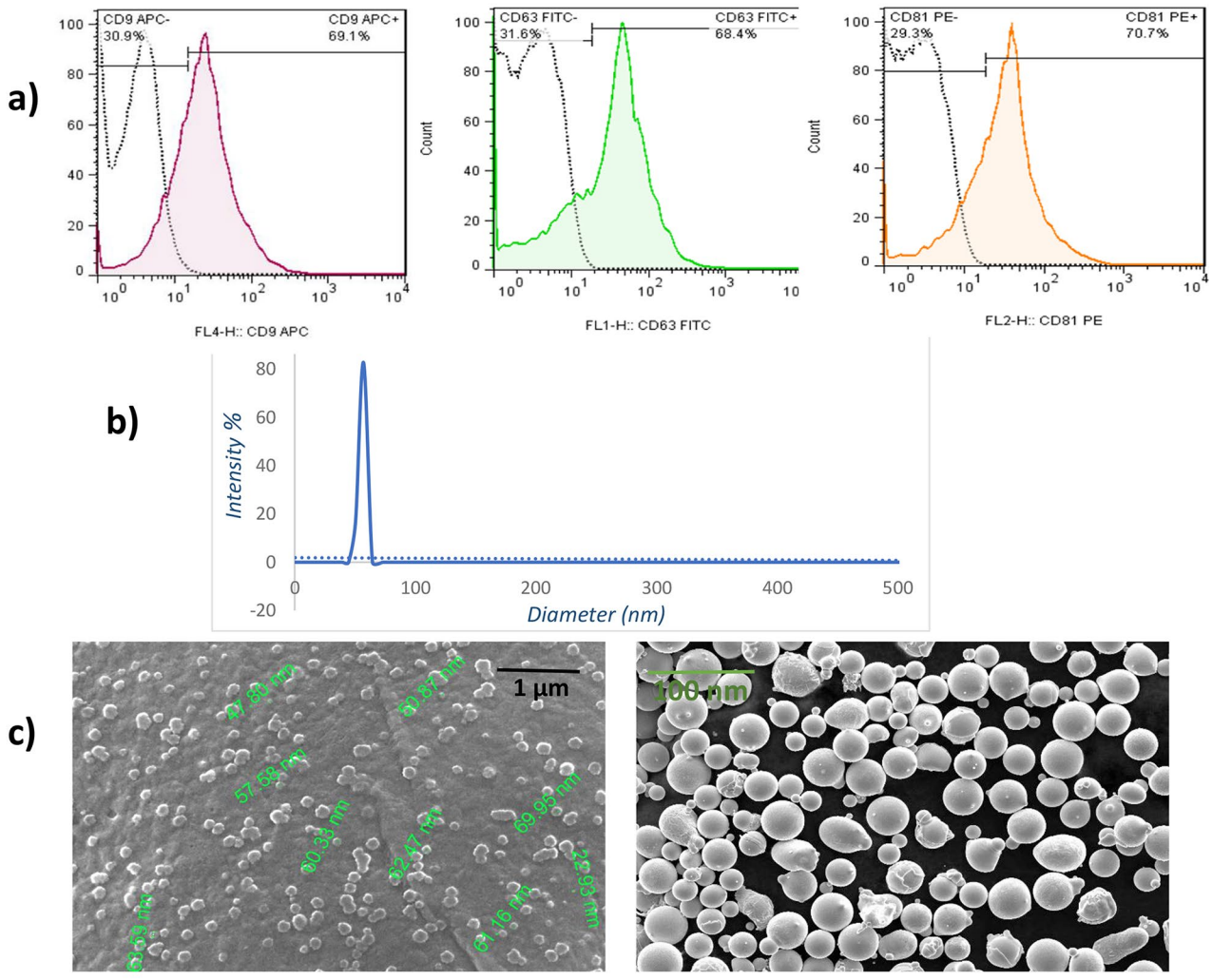

Fig. 3 Characterization of WJ-MSCs derived exosomes (**a**) The expression of the marker molecules CD9, CD63, and CD81 in the exosomes by flow cytometry. (**b**) The particle size distribution of exosomes by dynamic light scattering. (**c**) Morphology of exosomes observed under field emission scanning electron microscopy

percentage of cell viability and proliferation was increased in the groups treated with different concentrations of exosomes compared with the untreated control group after 24 h hypoxia and subsequent reoxygenation for 24, 48, and 72 h. As shown in Fig. 6a, our data demonstrated that the proliferation rate of conditioned HEK-293 cells has significantly enhanced by the highest concentration of 150 µg/ml WJ-MSC-EX$^{miR-210}$ for all post-hypoxia exposure time when compared with the untreated control cells (*$P<0.05$, **$P<0.01$, ***$P<0.001$,****$P<0.0001$).

Cell migration plays a pivotal role in the initial stages of angiogenesis. Cells are required to move or migrate towards the location where new blood vessel formation occurs [50]. The scratch test was carried out to explore the potential effect of preconditioned WJ-MSCs-EX$^{miR-210}$ on cell migration. As illustrated in Fig. 6b & c, apparent improvement in HEK-293 migration percentage was observed following the treatment with WJ-MSC-EX$^{miR-210}$ for 72 h at 50 µg/ml (60.88% ± 1.03), 100 µg/ml (76.17%± 0.95), and 150 µg/ml (82.00% ± 0.09) concentrations compared with the untreated cells (49.02%±1.93) ($P<0.05$).

ROS scavenging effect of WJ-MSC-EX$^{mir-210}$ on the injured kidney cells

The content of ROS was measured using DCFH-DA through flow cytometry. As shown in Fig. 7, the HEK-293 cells subjected to hypoxia condition exhibited an increase in DCF fluorescence, revealing excessive ROS content (89.10% ± 0.25) compared to normal cells (6.06% ± 0.50); however, treatment by WJ-MSC-EX$^{miR-210}$ decreased the DCF fluorescence intensity and ROS percentage for 50, 100 and 150 µg/ml in a concentration-dependent manner

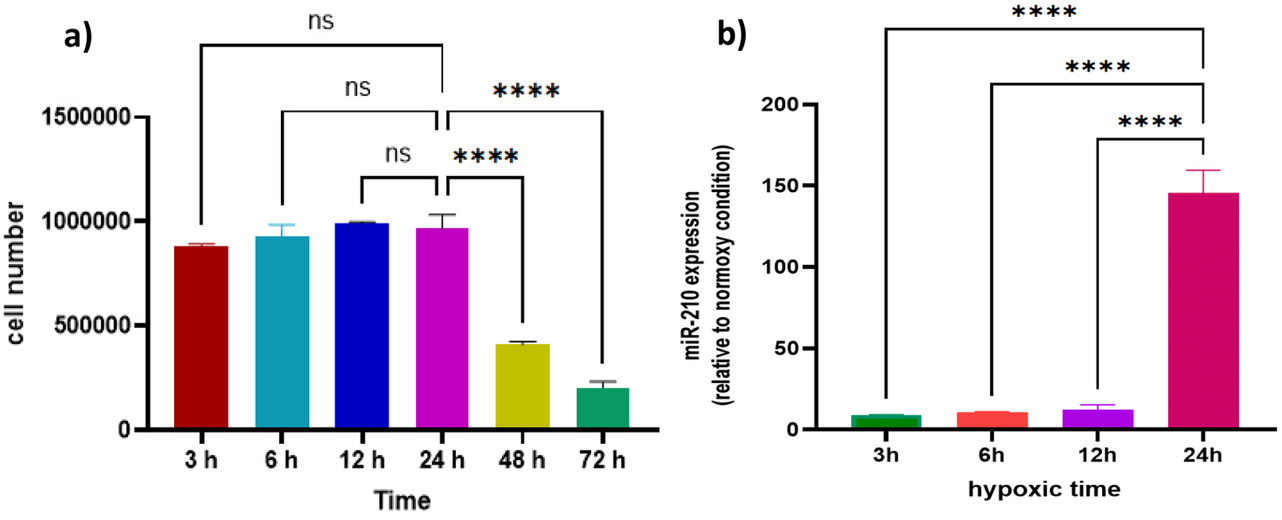

Fig. 4 Hypoxia preconditioning effect on cell viability and miR-210 expression in WJ-MSCs derived exosomes: (**a**) viability of WJ-MSCs 2D cells in different time of hypoxia condition (3,6, 12, 24, 48, and 72 h) from the same cell seeding number (0.8×10^6 WJ-MSCs), (**b**) changes in miR-210 expression by hypoxia duration in exosome derived WJ-MSCs spheroids

(18.30% ± 0.25, 9.84% ± 0.37, and 6.64% ± 0.70, respectively) ($P<0.05$).

Anti-apoptotic and viability-enhancing effects of WJ-MSC-EX$^{miR-210}$ on H/R kidney cells

As shown in Fig. 8, compared with the normoxic control group, the apoptosis rate increased after 24 hypoxia conditions (16.90% ± 0.36 vs. 1.57% ± 0.03). Interestingly, WJ-MSCs-EX$^{miR-210}$ decreased early apoptosis in a concentration-dependent manner so that the apoptosis percentage decreased from 37.4% ± 0.36 for untreated H/R cells to 28.4% ± 0.2, 25.2% ± 0.5, and 22.7% ± 0.1 ($P<0.05$) for the treated cells with 50 µg/ml, 100 µg/ml and 150 µg/ml WJ-MSC-EX$^{miR-210}$, respectively. In addition, treatment by WJ-MSCs-EX$^{miR-210}$ markedly enhanced the viability percentage in the H/R renal cells (Fig. 8), compared to untreated H/R cells (58.10% ± 0.95%), in a concentration-dependent manner (66.50% ± 0.70, 69.30% ± 0.75, 76.40% ± 1.00% for 50,100, and 150 µg/ml WJ-MSCs-EX$^{miR-210}$, respectively) ($P<0.05$).

Discussion

In recent decades, the importance of MSCs-based cell therapies for IRI lies in their multifaceted therapeutic effects, which target various aspects of the injury and promote tissue repair and regeneration [51, 52]. Also, experimental and clinical data suggest that MSC-derived exosomes could serve as innovative cell-free therapeutic agents, offering distinct advantages over MSCs [53]. The low yield of exosome derived MSCs, poses a challenge for scaling up the manufacturing of cell-free therapies. Therefore, researchers have explored different methods to enhance the production of them, such as refining MSC growth conditions, utilizing three-dimensional culture of MSCs, and controlling the process of exosome biogenesis [25]. So, we combined advantages of hypoxic MSCs preconditioning and 3D culture to improve yield and function of WJ-MSCs derived exosomes in IRI. Reality, hypoxic preconditioning of MSCs has been shown to improve the secretion [54] and the therapeutic efficacy of MSC-derived exosomes for tissue regeneration [55, 56] and various IRI diseases, including conditions characterized by ischemia and inadequate vessel growth in different tissues [57–59].

Accordingly, we used a comfortable and straightforward hypoxia preconditioning of the cells method, for the first time, to introduce miR-210 cargo in the exosomes derived from WJ-MSCs. In addition, hypoxia treating of WJ-MSCs prepare them to encounter low oxygen and nutrient-limited condition in 3D culture [60] that increased cell viability in spheroids (Fig. 2c & d). Also, as shown in Fig. 2e and a, 3D culture of WJ-MSCs improved the yield of exosome secretion by about 3-fold compared to a 2D culture. Consistent with our reports, it is shown by Cao et al. that revealed exosomes derived from MSCs in a 3D culture setting yielded greater quantities. These exosomes exhibited high anti-inflammatory properties, offering protection against cisplatin-induced kidney injury [61].

Apart from the exosome yield, our study provides confirmation of the enhanced effects of hypoxia on the action of WJ-MSC secreted exosomes through overexpression of miR-210 cargo (Fig. 4b). miR-210 is recognized as the main mediator of the cellular response to hypoxic stress. A diverse range of targets regulated by miR-210 have been implicated in mitochondrial metabolism [62], oxidative stress responses [63], cell proliferation [64], and regulating cell death or apoptosis [65]. These regulatory

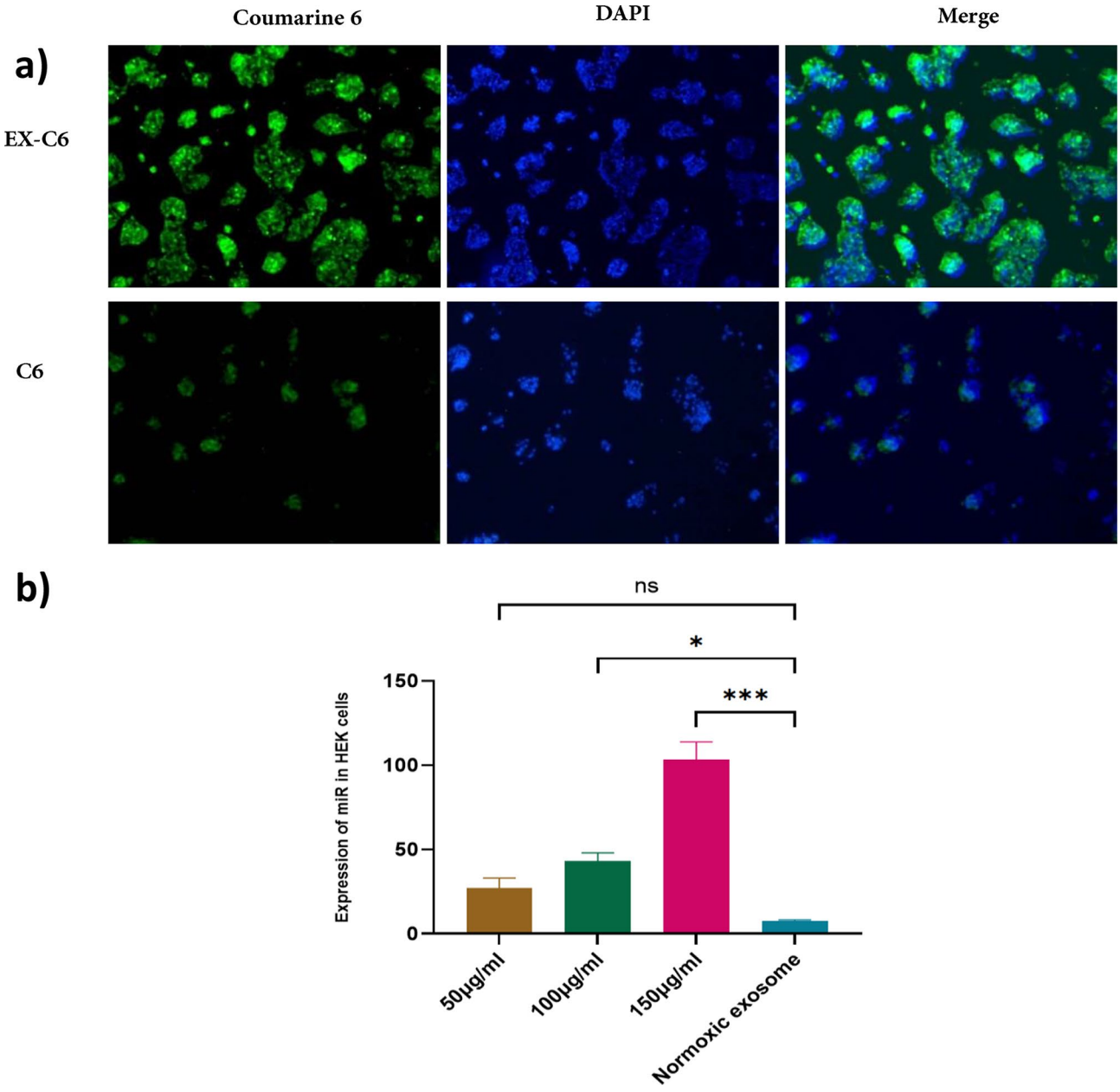

Fig. 5 Internalize of exosome derived hypoxia treated WJ-MSCs in H/R renal cells; (**a**) Fluorescent microscopy images in 10X of IRI HEK-293 cells treated with the coumarin-6 loaded exosomes (EX-C6) and free coumarin-6 (C6) solution after 4 h incubation at 37 °C. Green fluorescence signals indicated the presence of coumarin-6, while the blue fluorescence signals corresponded to the DAPI-stained cellular nuclei. (**b**) miR-210 expression in IRI HEK-293 cells treated by hypoxic and normoxic exosomes vs. untreated one; (*$P < 0.05$, **$P < 0.01$, ***$P < 0.001$, ****$P < 0.0001$)

effects have broad implications across various pathological conditions, including cancer and IRI. Remarkably, in a mouse model of renal I/R injury, miR-210 was found to be upregulated in kidney tissue [66]. Therefore, we demonstrated that exosomes with miR-210 overexpression (WJ-MSC-EX$^{miR-210}$) have a protective role in renal cells, mitigating injury and dysfunction induced by hypoxia/reoxygenation (H/R). Our findings in Fig. 5b indicated that WJ-MSC-EX$^{miR-210}$ incorporated by HEK cells and notably boost their proliferation and migration capabilities (Fig. 6b & c). Both cell migration and proliferation, which play critical roles in alleviating renal IRI and facilitating tissue repair [50], that enhanced by exosomes derived from hypoxia preconditioned MSCs [67–70]. Also, in other literatures, the elevated expression of miR-210 notably increased VEGF levels and promoted the proliferation and migration of different cells [71–74]. Moreover, in vivo studies indicated improved tissue function, and these beneficial effects were correlated with alterations in the expression of miR-210

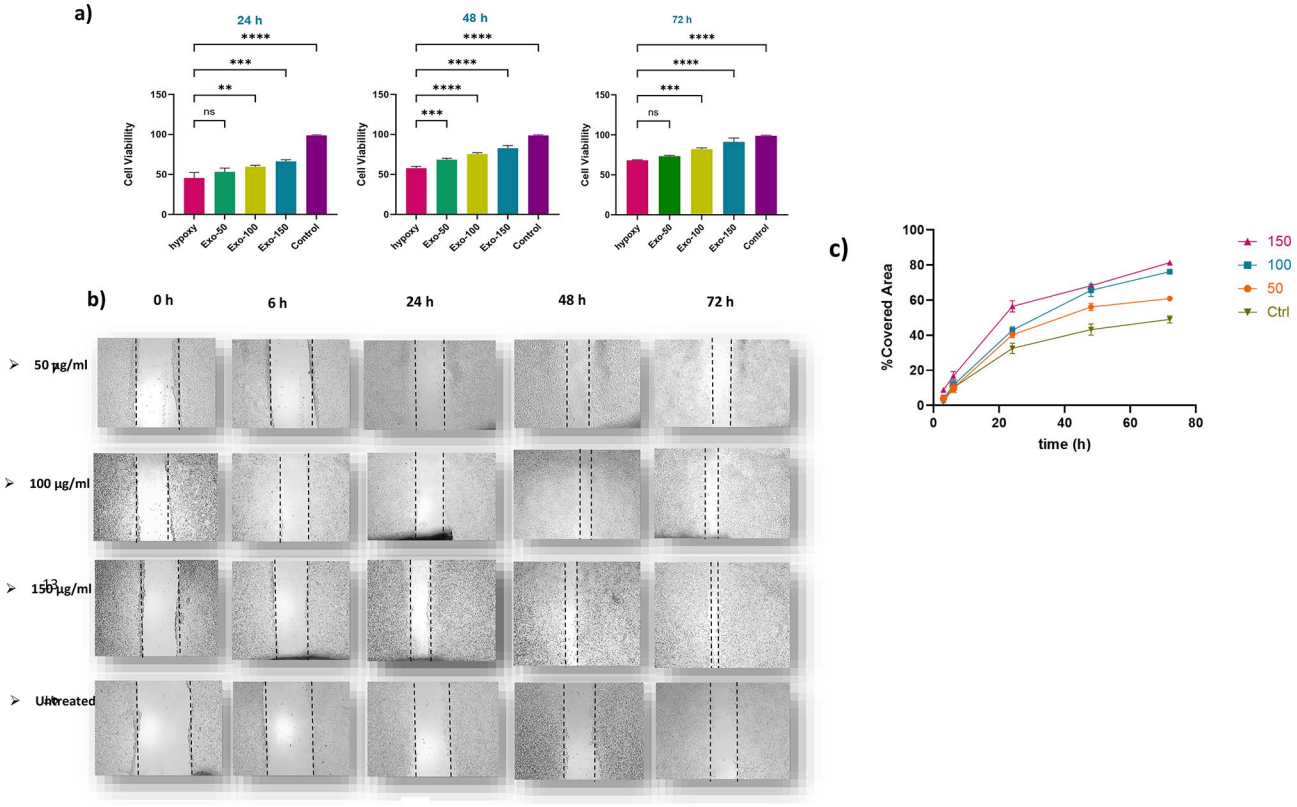

Fig. 6 WJ-MSC- $EX^{miR-210}$ alters migration and viability of renal cells: (**a**) Renal cell viability results via MTT test in 24, 48, and 72 h after treatment by various amounts of WJ-MSCs-$EX^{miR-210}$. (**b**) Increased migration of HEK-293 cells through treatment by different concentrations of WJ-MSC- $EX^{miR-210}$ (50, 100, and 150 µg/ml) at various times (0,6,24,48 and 72 h); (**c**) The migration rate of cells was assessed based on the distance of the selected scratch area at each time intervals of 0,6,24,48 and 72 h, and the percentage of scratch closure was determined for each time point by Image J software ($n = 3$, mean ± SD)

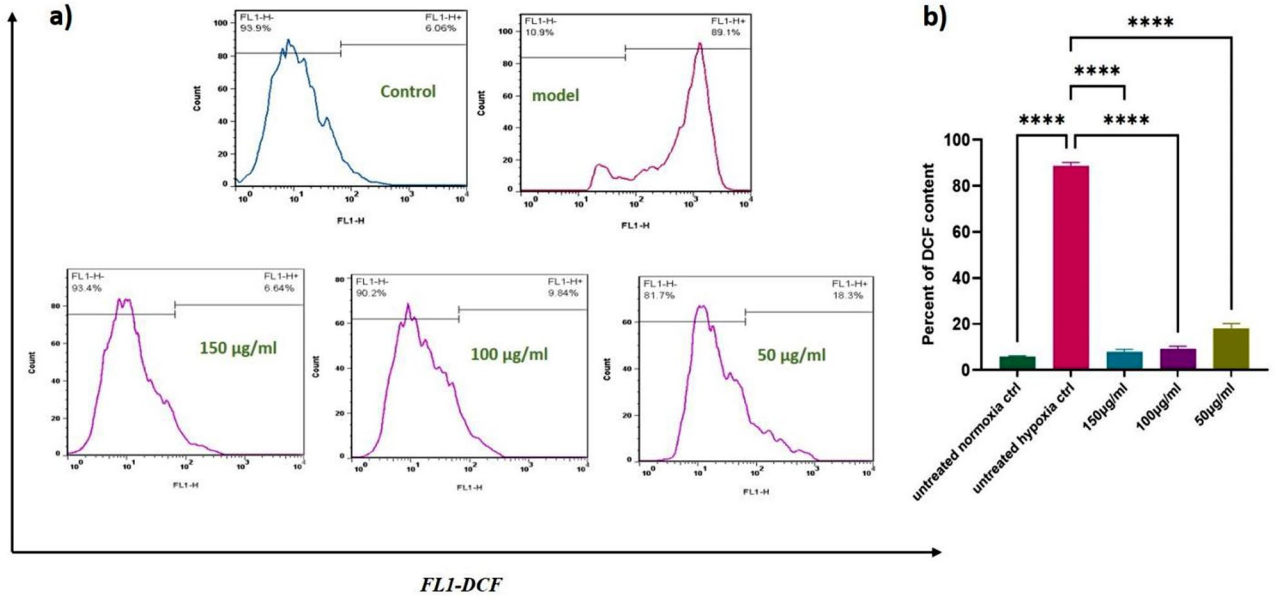

Fig. 7 In vitro reactive oxygen species (ROS) assay via DCFH-DA flow cytometry; (**a**) in HEK-293 cells; untreated normoxia condition (control), untreated hypoxia condition (model), hypoxia conditioned HEK-293 cells treated by different concentrations of WJ-MSC-$EX^{miR-210}$ (50,100 and 150 µg/ml, respectively). (**b**) the percent of DCF content in renal cells

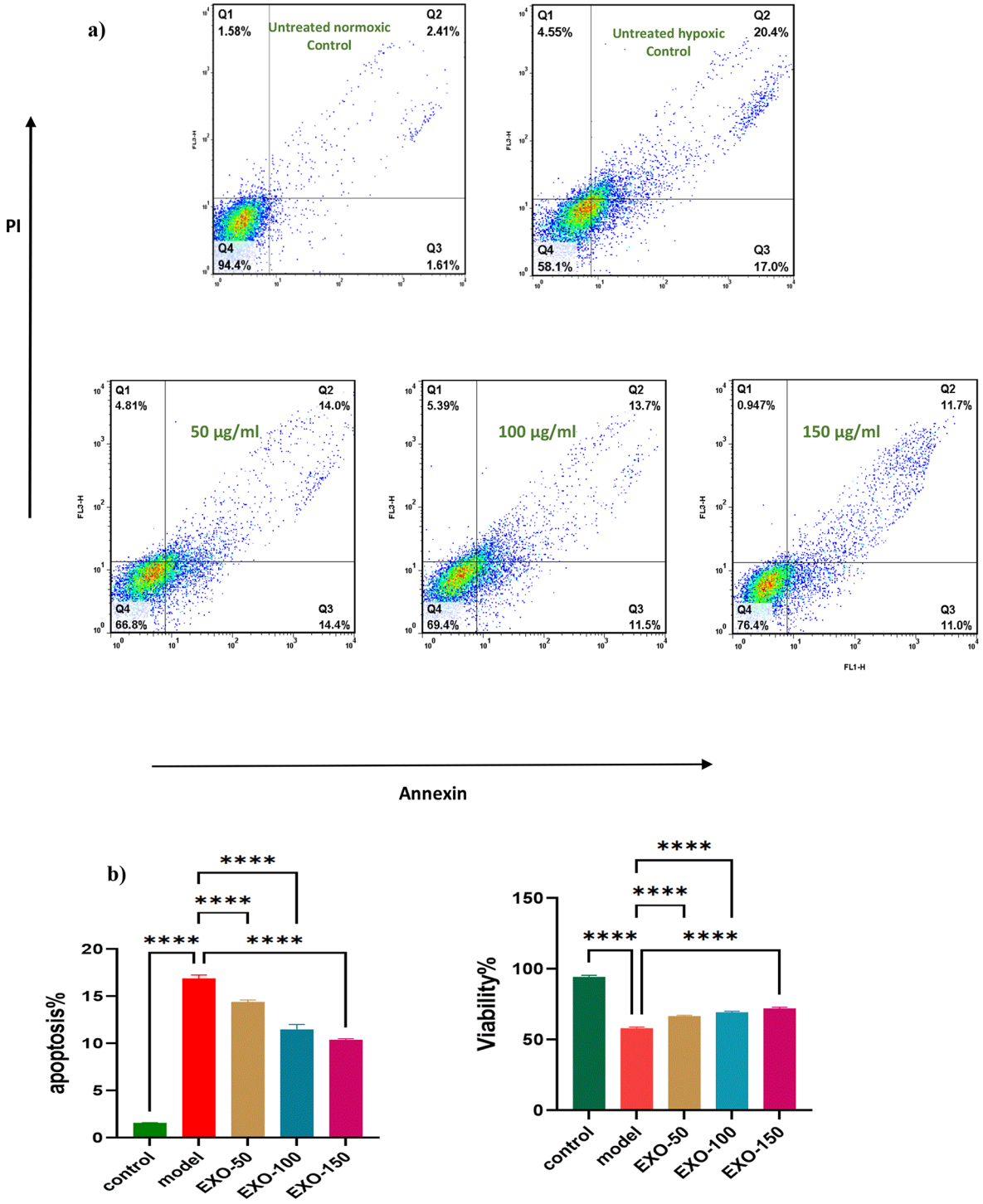

Fig. 8 Apoptosis and cell viability assays: (**a**) Annexin V (FL1-H) and propidium iodide (FL3-H) staining were employed to identify distinct H/R HEK-293 cell populations. Within each panel, the lower left quadrant, characterized by FITC-Annexin V negativity and PI negativity, represents viable cells. The lower right quadrant, marked by FITC-Annexin positivity and PI negativity, indicates cells in the early stages of apoptosis. Conversely, the upper left and upper right quadrants, which are stained with PI (PI positive), signify dead cells; (**b**) the percentage of cell viability and apoptosis for different WJ-MSC-EX$^{miR-210}$ concentrations (50,100, and 150 µg/ml) following 24 h treatment. (****$P < 0.0001$)

target genes, specifically PI3K/Akt and p53 [75]. The protein p53, which directly binds to the miR-210 promoter, governs critical cellular processes like apoptosis, and it also mitigates inflammation in diverse human tissues in response to stress conditions [76]. In present work, we revealed that treatment with WJ-MSC-EX$^{miR-210}$ enhanced survival and reduced apoptosis of HEK-293 cell under H/R conditions in vitro (Figs. 6a and 8). These findings show that increased concentration of WJ-MSC-EX$^{miR-210}$, lead to elevating miR-210 expression levels in renal cells, improving he viability of injured renal cells and the incidence of apoptosis is reduced. In accordance with our results about anti-apoptotic role of miR-210, Liu et al. proved the overexpression of miR-210 resulted in a notable inhibition of the HIF-1α pathway and reduced apoptosis induced by hypoxia kidney lesions. Conversely, knockdown of miR-210 had the opposite effect, exacerbating apoptosis [77]. Zaccagnini and colleagues documented that miR-210 played a critical role in the adaptive mechanism for regulating oxidative metabolism and oxidative stress in acute peripheral ischemia [78]. Also, it is documented that miR-210 diminishes apoptosis by impeding the caspase-8 pathway in H_2O_2-stimulated human umbilical vein endothelial cells [79]. Our flow cytometry apoptosis/necrosis in Fig. 8 results in accordance with these investigations confirm that miR-210 overexpressed in preconditioned WJ-MSC derived exosomes exert a protective function in H/R renal cells in vitro.

Oxidative stress, recognized as a predominant pathological mechanism in IRI, denotes a disparity between the regular oxidant defense systems, encompassing enzymes like superoxide dismutase, catalase, and glutathione, and the generation of intracellular ROS. This imbalance culminates in accumulating detrimental reactive oxygen intermediates, including hydrogen peroxide (H_2O_2) [80]. In this work, according to the flow cytometry ROS assessment (Fig. 7), the WJ-MSCs-EX$^{miR-210}$ remarkably diminishes the ROS content in H/R kidney cells. Under typical physiological circumstances, ROS arise from routine cellular metabolic activities and are counterbalanced by antioxidants, maintaining a homeostatic equilibrium [81]. However, ROS generation is enhanced during the ischemic phase and subsequent reperfusion, exacerbating oxidative stress and cellular damage [82]. Different findings suggest that MSCs-derived exosomes may exert their effects by enhancing antioxidant mechanisms and suppressing oxidative stress within injured renal tissues. For instance, Bo Liu and colleagues propose the potential therapeutic use of human umbilical cord mesenchymal stem cells in CKD. The mechanism of action was linked to the suppression of the ROS-mediated p38MAPK/ERK signaling pathway [83]. In another study, Cao et al. demonstrated that coculturing with MSC-derived extracellular vesicles led to a reduction in ROS levels in renal proximal tubular epithelial cells. This antioxidant effect was mediated by the activation of the Keap1-Nrf2 signaling pathway [84]. Also, Mutharasan et al. found that upregulation of miR-210 decreased ROS production and cardiomyocytes death in reaction to oxidative stress, whereas the downregulation of miR-210 resulted in elevated ROS levels following hypoxia-reoxygenation [85].

Additionally, ROS signaling is pivotal in the initiation and progression of inflammatory injuries [86]. MSC-EX has demonstrated the capability to mitigate inflammatory injuries triggered by oxidative stress within tissues. Notably, in literatures were showed treatment with MSC-EVs attenuated the levels of inflammatory cytokines, indicating a potential therapeutic role in mitigating renal injury [87, 88]. Furthermore, many researches illustrate an immunomodulatory function of miR-210 [89–91] that improved immunosuppressive effect of MSCs EX in IRI model. For instance, Xie et al. demonstrated that mesenchymal stem cell-derived exosomes may improve kidney injury by facilitating the transition of M1 macrophages to M2 macrophages and exerting anti-inflammatory effects through M2 macrophages. This suggests that the immunomodulatory properties of MSCs-Exo play a role in the self-repair process in mice following ischemia-reperfusion injury [92].

Conclusion

Our study suggests that combined hypoxic preconditioning and 3D spheroid culture of WJ-MSCs enhances cell survival in 3D culture conditions, increasing secretion of exosomes and expression of miR-210 payload. Interestingly, WJ-MSC-EX$^{miR-210}$ increased the level of miR-210 in the H/R kidney cells. In addition, our findings revealed that WJ-MSC-EX$^{miR-210}$ can boost the protective properties against apoptosis, oxidative stress, and reduced injury induced by the H/R condition. Further research is warranted to determine WJ-MSC-EX$^{miR-210}$ impact on renal ischemia-reperfusion injury in vivo.

Acknowledgements

We acknowledge the Center for Nanotechnology in Drug Delivery (SUMS) for providing the research facilities. Additionally, we express our gratitude to Prof. Hossein Mirhendi, Director of the Core Research Facility (CRF) at Isfahan University of Medical Sciences, Iran, for permitting us to conduct the cell culture experiments. The authors declare that they have not used AI-generated work in this manuscript.

Author contributions

Ali Mohammad Tamaddon and Samira Sadat Abolmaali co-supervised the project. Ali Mohammad Tamaddon, Vajihe Azimian Zavareh, and Reyhane Toghiani designed the study. Reyhane Toghiani and Haniyeh Najafi carried out the experiments. Negar Azarpira provided the techniques for the isolation and characterization of WJ-MSCs. Ali Mohammad Tamaddon and Reyhaneh Toghiani analyzed the data. Jaleh Varshosaz and Mina Mirian provided invaluable comments and suggestions. Reyhane Toghiani wrote

the manuscript. Ali Mohammad Tamaddon, Samira Sadat Abolmaali, Jaleh Varshosaz, Haniyeh Najafi, and Mina Mirian revised the manuscript. All authors have read and approved the final manuscript.

Funding
The study was funded by Shiraz University of Medical Sciences (Grant No: 24884).

Data availability
Not applicable.

Declarations

Ethics approval and consent to participate
(1) The project title: Hybrid Exosomes Derived from Mesenchymal Stem Cells Delivering Antioxidant Cargos for Renal Ischemia-Reperfusion Injury; (2) Name of the institutional approval committee: Research Ethics Committee at Shiraz University of Medical Sciences (SUMS); (3) The approval number: IR.SUMS.REC.1401.443; (4) The approval date: Oct 3, 2022. Written informed consent was received from mothers for the collection of umbilical cord blood stem cells.

Consent for publication
Not applicable.

Competing interests
The authors declare there is no competing interest.

Received: 9 April 2024 / Accepted: 11 July 2024
Published online: 30 July 2024

References

1. Shiva N, et al. Renal ischemia/reperfusion injury: an insight on in vitro and in vivo models. Life Sci. 2020;256:117860.
2. Ali M, et al. Extracellular vesicles for treatment of solid organ ischemia–reperfusion injury. Am J Transplant. 2020;20(12):3294–307.
3. Kalogeris T, et al. Cell biology of ischemia/reperfusion injury. Int Rev cell Mol Biology. 2012;298:229–317.
4. Kalogeris T, et al. Ischemia/reperfusion. Compr Physiol. 2016;7(1):113.
5. Barzegar M, et al. Potential therapeutic roles of stem cells in ischemia-reperfusion injury. Stem cell Res. 2019;37:101421.
6. Gao J, et al. The dynamic in vivo distribution of bone marrow-derived mesenchymal stem cells after infusion. Cells Tissues Organs. 2001;169(1):12–20.
7. Togel F, et al. Administered mesenchymal stem cells protect against ischemic acute renal failure through differentiation-independent mechanisms. Am J Physiology-Renal Physiol. 2005;289(1):F31–42.
8. Emanueli C, et al. Exosomes and exosomal miRNAs in cardiovascular protection and repair. Vascul Pharmacol. 2015;71:24–30.
9. Izadpanah M, et al. Potential of extracellular vesicles in neurodegenerative diseases: diagnostic and therapeutic indications. J Mol Neurosci. 2018;66:172–9.
10. Li JJ, et al. Stem cell-derived extracellular vesicles for treating joint injury and osteoarthritis. Nanomaterials. 2019;9(2):261.
11. Han C, et al. Extracellular vesicles in cardiovascular disease: Biological functions and therapeutic implications. Pharmacol Ther. 2022;233:108025.
12. Eirin A, et al. Mesenchymal stem cell–derived extracellular vesicles attenuate kidney inflammation. Kidney Int. 2017;92(1):114–24.
13. Ding J-Y, et al. Mesenchymal stem cell-derived extracellular vesicles in skin wound healing: roles, opportunities and challenges. Military Med Res. 2023;10(1):36.
14. Brigstock DR. Extracellular vesicles in organ fibrosis: mechanisms, therapies, and diagnostics. Cells. 2021;10(7):1596.
15. Wei H, et al. Regulation of exosome production and cargo sorting. Int J Biol Sci. 2021;17(1):163.
16. Di Bella MA. Overview and update on extracellular vesicles: considerations on exosomes and their application in modern medicine. Biology. 2022;11(6):804.
17. He J, et al. Exosomal targeting and its potential clinical application. Drug Delivery Translational Res. 2022;12(10):2385–402.
18. Mardpour S, et al. Interaction between mesenchymal stromal cell-derived extracellular vesicles and immune cells by distinct protein content. J Cell Physiol. 2019;234(6):8249–58.
19. Pan Y, et al. Mesenchymal stem cell-derived exosomes in cardiovascular and cerebrovascular diseases: from mechanisms to therapy. Volume 163. Biomedicine & Pharmacotherapy; 2023. p. 114817.
20. Ranjan P, et al. Challenges and future scope of exosomes in the treatment of cardiovascular diseases. The Journal of Physiology; 2022.
21. Toghiani R, et al. Bioengineering exosomes for treatment of organ ischemia-reperfusion injury. Life Sci. 2022;302:120654.
22. Zheng Q, et al. The unique immunomodulatory properties of MSC-derived exosomes in organ transplantation. Front Immunol. 2021;12:659621.
23. Akyurekli C, et al. A systematic review of preclinical studies on the therapeutic potential of mesenchymal stromal cell-derived microvesicles. Stem Cell Reviews Rep. 2015;11:150–60.
24. Oveili E, et al. The potential use of mesenchymal stem cells-derived exosomes as microRNAs delivery systems in different diseases. Cell Communication Signal. 2023;21(1):1–26.
25. Phan J, et al. Engineering mesenchymal stem cells to improve their exosome efficacy and yield for cell-free therapy. J Extracell Vesicles. 2018;7(1):1522236.
26. Haraszti RA, et al. Exosomes produced from 3D cultures of MSCs by tangential flow filtration show higher yield and improved activity. Mol Ther. 2018;26(12):2838–47.
27. Yan L, Wu X. Exosomes produced from 3D cultures of umbilical cord mesenchymal stem cells in a hollow-fiber bioreactor show improved osteochondral regeneration activity. Cell Biol Toxicol. 2020;36:165–78.
28. Luo Y, et al. Characteristics of culture-condition stimulated exosomes or their loaded hydrogels in comparison with other extracellular vesicles or MSC lysates. Front Bioeng Biotechnol. 2022;10:1016833.
29. Fiedler J, et al. MicroRNA-24 regulates vascularity after myocardial infarction. Circulation. 2011;124(6):720–30.
30. Peng Y, et al. Exosomal mir-25-3p from mesenchymal stem cells alleviates myocardial infarction by targeting pro-apoptotic proteins and EZH2. Cell Death Dis. 2020;11(5):317.
31. Cantaluppi V, et al. Microvesicles derived from endothelial progenitor cells protect the kidney from ischemia–reperfusion injury by microRNA-dependent reprogramming of resident renal cells. Kidney Int. 2012;82(4):412–27.
32. Devlin C, et al. miR-210: more than a silent player in hypoxia. IUBMB Life. 2011;63(2):94–100.
33. Zhang H, et al. Exosome-mediated targeted delivery of miR-210 for angiogenic therapy after cerebral ischemia in mice. J Nanobiotechnol. 2019;17:1–13.
34. Lou Y-L, et al. miR-210 activates notch signaling pathway in angiogenesis induced by cerebral ischemia. Mol Cell Biochem. 2012;370:45–51.
35. Zaccagnini G, et al. miR-210 hypoxamiR in Angiogenesis and Diabetes. Antioxid Redox Signal. 2022;36(10):685–706.
36. Shi Y-F, et al. Insulin protects H9c2 rat cardiomyoblast cells against hydrogen peroxide-induced injury through upregulation of microRNA-210. Free Radic Res. 2015;49(9):1147–55.
37. Diao H, et al. MicroRNA-210 alleviates oxidative stress-associated cardiomyocyte apoptosis by regulating BNIP3. Biosci Biotechnol Biochem. 2017;81(9):1712–20.
38. Tamaddon AM et al. Biocompatibility of graphene oxide nanosheets functionalized with various amino acids towards mesenchymal stem cells. Heliyon, 2023. 9(8).
39. Khosravi M, et al. Differentiation of umbilical cord derived mesenchymal stem cells to hepatocyte cells by transfection of miR-106a, miR-574-3p, and miR-451. Gene. 2018;667:1–9.
40. Dominici M, et al. Minimal criteria for defining multipotent mesenchymal stromal cells. The International Society for Cellular Therapy position statement. Cytotherapy. 2006;8(4):315–7.
41. Matthiesen S, Jahnke R, Knittler MR. A straightforward hypoxic cell culture method suitable for standard incubators. Methods Protocols. 2021;4(2):25.
42. Kim M, et al. Three-dimensional spheroid culture increases exosome secretion from mesenchymal stem cells. Tissue Eng Regenerative Med. 2018;15:427–36.
43. Bank HL. Rapid assessment of islet viability with acridine orange and propidium iodide. vitro Cell Dev Biology. 1988;24(4):266–73.
44. Ashour AA, et al. Luteolin-loaded exosomes derived from bone marrow mesenchymal stem cells: a promising therapy for liver fibrosis. Drug Delivery. 2022;29(1):3270–80.

45. Kumar DN, et al. Combination therapy comprising paclitaxel and 5-fluorouracil by using folic acid functionalized bovine milk exosomes improves the therapeutic efficacy against breast cancer. Life. 2022;12(8):1143.
46. Moraes DA, et al. A reduction in CD90 (THY-1) expression results in increased differentiation of mesenchymal stromal cells. Stem Cell Res Ther. 2016;7:1–14.
47. Parsekar SU, et al. Protein binding studies with human serum albumin, molecular docking and in vitro cytotoxicity studies using HeLa cervical carcinoma cells of Cu (II)/Zn (II) complexes containing a carbohydrazone ligand. Dalton Trans. 2020;49(9):2947–65.
48. Chopra N, et al. Biophysical characterization and drug delivery potential of exosomes from human Wharton's jelly-derived mesenchymal stem cells. ACS Omega. 2019;4(8):13143–52.
49. Donoso-Quezada J, Ayala-Mar S, González-Valdez J. The role of lipids in exosome biology and intercellular communication: function, analytics and applications. Traffic. 2021;22(7):204–20.
50. Adair TH, Montani J-P. Angiogenesis 2011.
51. Oliva J. Therapeutic properties of mesenchymal stem cell on organ ischemia-reperfusion injury. Int J Mol Sci. 2019;20(21):5511.
52. Hu H, Zou C. Mesenchymal stem cells in renal ischemia-reperfusion injury: biological and therapeutic perspectives. Curr Stem Cell Res Therapy. 2017;12(3):183–7.
53. Yin K, Wang S, Zhao RC. Exosomes from mesenchymal stem/stromal cells: a new therapeutic paradigm. Biomark Res. 2019;7:1–8.
54. Li H, et al. Hypoxia and inflammatory factor preconditioning enhances the immunosuppressive properties of human umbilical cord mesenchymal stem cells. World J Stem Cells. 2023;15(11):999.
55. Ferreira JR, et al. Mesenchymal stromal cell secretome: influencing therapeutic potential by cellular pre-conditioning. Front Immunol. 2018;9:2837.
56. Pendse S, Kale V, Vaidya A. Extracellular vesicles isolated from mesenchymal stromal cells primed with hypoxia: novel strategy in regenerative medicine. Curr Stem Cell Res Therapy. 2021;16(3):243–61.
57. Gonzalez-King H, et al. Hypoxia inducible factor-1α potentiates jagged 1-mediated angiogenesis by mesenchymal stem cell-derived exosomes. Stem Cells. 2017;35(7):1747–59.
58. Zhu L-P, et al. Hypoxia-elicited mesenchymal stem cell-derived exosomes facilitates cardiac repair through miR-125b-mediated prevention of cell death in myocardial infarction. Theranostics. 2018;8(22):6163.
59. Liu W, et al. Exosome-shuttled miR-216a-5p from hypoxic preconditioned mesenchymal stem cells repair traumatic spinal cord injury by shifting microglial M1/M2 polarization. J Neuroinflamm. 2020;17(1):1–22.
60. Peck SH, et al. Hypoxic preconditioning enhances bone marrow–derived mesenchymal stem cell survival in a low oxygen and nutrient-limited 3D microenvironment. Cartilage. 2021;12(4):512–25.
61. Cao J, et al. Three-dimensional culture of MSCs produces exosomes with improved yield and enhanced therapeutic efficacy for cisplatin-induced acute kidney injury. Stem Cell Res Ther. 2020;11:1–13.
62. Chan SY, et al. MicroRNA-210 controls mitochondrial metabolism during hypoxia by repressing the iron-sulfur cluster assembly proteins ISCU1/2. Cell Metabol. 2009;10(4):273–84.
63. Ivan M, Huang X. miR-210: fine-tuning the hypoxic response Tumor Microenvironment and Cellular Stress: Signaling, Metabolism, Imaging, and Therapeutic Targets, 2014: pp. 205–227.
64. Zhang S, et al. MicroRNA-210 regulates cell proliferation and apoptosis by targeting regulator of differentiation 1 in glioblastoma cells. Folia Neuropathol. 2015;53(3):236–44.
65. Marwarha G, et al. miR-210 regulates apoptotic cell death during cellular hypoxia and reoxygenation in a diametrically opposite manner. Biomedicines. 2021;10(1):42.
66. Lorenzen JM, Thum T. Circulating and urinary microRNAs in kidney disease. Clin J Am Soc Nephrol. 2012;7(9):1528–33.
67. Ferreira AdF et al. Extracellular vesicles from adipose-derived mesenchymal stem/stromal cells accelerate migration and activate AKT pathway in human keratinocytes and fibroblasts independently of miR-205 activity Stem cells international, 2017. 2017.
68. Shabbir A, et al. Mesenchymal stem cell exosomes induce proliferation and migration of normal and chronic wound fibroblasts, and enhance angiogenesis in vitro. Stem Cells Dev. 2015;24(14):1635–47.
69. Ye Y-C, et al. Infarct-preconditioning exosomes of umbilical cord mesenchymal stem cells promoted vascular remodeling and neurological recovery after stroke in rats. Stem Cell Res Ther. 2022;13(1):1–15.
70. Liang L, et al. Exosomes derived from human umbilical cord mesenchymal stem cells repair injured endometrial epithelial cells. J Assist Reprod Genet. 2020;37:395–403.
71. Zheng Z, et al. Adipose-derived stem cell-derived microvesicle-released miR-210 promoted proliferation, migration and invasion of endothelial cells by regulating RUNX3. Cell Cycle. 2018;17(8):1026–33.
72. Arif M, et al. MicroRNA-210-mediated proliferation, survival, and angiogenesis promote cardiac repair post myocardial infarction in rodents. J Mol Med. 2017;95:1369–85.
73. Wang J, et al. Huoxue Anxin recipe (活血安心方) promotes myocardium angiogenesis of acute myocardial infarction rats by up-regulating miR-210 and vascular endothelial growth factor. Chin J Integr Med. 2016;22:685–90.
74. Liu F, et al. Upregulation of microRNA-210 regulates renal angiogenesis mediated by activation of VEGF signaling pathway under ischemia/perfusion injury in vivo and in vitro. Kidney Blood Press Res. 2012;35(3):182–91.
75. Cheng H, et al. Hypoxia-challenged MSC-derived exosomes deliver miR-210 to attenuate post-infarction cardiac apoptosis. Stem Cell Res Ther. 2020;11(1):1–14.
76. Barabutis N, Schally AV, Siejka A. P53, GHRH, inflammation and cancer. EBioMedicine. 2018;37:557–62.
77. Liu L-L, et al. miR-210 protects renal cell against hypoxia-induced apoptosis by targeting HIF-1 alpha. Mol Med. 2017;23:258–71.
78. Zaccagnini G, et al. Hypoxia-induced miR-210 modulates tissue response to acute peripheral ischemia. Antioxid Redox Signal. 2014;21(8):1177–88.
79. Li T et al. Protection of human umbilical vein endothelial cells against oxidative stress by MicroRNA-210 Oxidative medicine and cellular longevity, 2017. 2017.
80. Chazelas P, et al. Oxidative stress evaluation in ischemia reperfusion models: characteristics, limits and perspectives. Int J Mol Sci. 2021;22(5):2366.
81. Sharifi-Rad M, et al. Lifestyle, oxidative stress, and antioxidants: back and forth in the pathophysiology of chronic diseases. Front Physiol. 2020;11:694.
82. Raedschelders K, Ansley DM, Chen DD. The cellular and molecular origin of reactive oxygen species generation during myocardial ischemia and reperfusion. Volume 133. Pharmacology & therapeutics; 2012. pp. 230–55. 2.
83. Gao Z, et al. Hypoxic mesenchymal stem cell-derived extracellular vesicles ameliorate renal fibrosis after ischemia–reperfusion injure by restoring CPT1A mediated fatty acid oxidation. Stem Cell Res Ther. 2022;13(1):191.
84. Cao H, et al. In vivo tracking of mesenchymal stem cell-derived extracellular vesicles improving mitochondrial function in renal ischemia–reperfusion injury. ACS Nano. 2020;14(4):4014–26.
85. Mutharasan RK, et al. microRNA-210 is upregulated in hypoxic cardiomyocytes through akt-and p53-dependent pathways and exerts cytoprotective effects. Am J Physiol Heart Circ Physiol. 2011;301(4):H1519–30.
86. Kellner M et al. ROS signaling in the pathogenesis of acute lung injury (ALI) and acute respiratory distress syndrome (ARDS) Pulmonary vasculature redox signaling in health and disease, 2017: pp. 105–137.
87. Stallons LJ, Whitaker RM, Schnellmann RG. Suppressed mitochondrial biogenesis in folic acid-induced acute kidney injury and early fibrosis. Toxicol Lett. 2014;224(3):326–32.
88. West A et al. Mitochondrial DNA stress primes the antiviral innate immune response. Nature 520 (Apri (7548)), 553–557. 2015.
89. Wu R, et al. MicroRNA-210 overexpression promotes psoriasis-like inflammation by inducing Th1 and Th17 cell differentiation. J Clin Investig. 2018;128(6):2551–68.
90. Cicchillitti L, et al. Hypoxia-inducible factor 1-α induces miR-210 in normoxic differentiating myoblasts. J Biol Chem. 2012;287(53):44761–71.
91. Zaccagnini G, et al. Hypoxia-induced miR-210 modulates the inflammatory response and fibrosis upon acute ischemia. Cell Death Dis. 2021;12(5):435.
92. Xie X et al. Exosome from indoleamine 2, 3-dioxygenase-overexpressing bone marrow mesenchymal stem cells accelerates repair process of ischemia/reperfusion-induced acute kidney injury by regulating macrophages polarization Stem cell research & therapy, 2022. 13(1): p. 367.

Publisher's Note